Analysis of numerical methods for evaluating the Fock exchange integral in a plane wave basis

N. A. W. Holzwarth[*] and Xiao Xu

Department of Physics, Wake Forest University, Winston-Salem, North Carolina 27109, USA
(Dated: August 13, 2011)

In this brief report, we analyze methods for evaluating the singular integrals of the Fock exchange interaction with the help of a simple analytic model. We find that Brillouin zone sampling can be important even for systems with large unit cells.

I. INTRODUCTION

Recently, there has been a lot of interest in using "exact" Fock exchange in first-principles calculations in order to avoid electron self-interaction.[1–10] In terms of Bloch states $\Psi_{n\mathbf{k}}(\mathbf{r})$ of band index n and wavevector $\mathbf{k}$, the Fock exchange energy can be written in the form[11]

$$
\begin{aligned}
E_x = & -\frac{e^2}{4} \sum_{n\mathbf{k}n'\mathbf{k}'} f_{n\mathbf{k}} f_{n'\mathbf{k}'} \\
& \times \int d^3r \, d^3r' \frac{\rho_{n\mathbf{k},n'\mathbf{k}'}(\mathbf{r})\rho^*_{n\mathbf{k},n'\mathbf{k}'}(\mathbf{r}')}{|\mathbf{r}-\mathbf{r}'|} \\
= & -\frac{e^2\pi}{\mathcal{V}} \sum_{n\mathbf{k}n'\mathbf{k}'} f_{n\mathbf{k}} f_{n'\mathbf{k}'} \sum_{\mathbf{G}} \frac{|\overline{\rho}_{n\mathbf{k},n'\mathbf{k}'}(\mathbf{G})|^2}{|\mathbf{k}-\mathbf{k}'+\mathbf{G}|^2}.
\end{aligned}
\tag{1}
$$

Here, the pair density function is defined to be

$$
\rho_{n\mathbf{k},n'\mathbf{k}'}(\mathbf{r}) \equiv \Psi_{n\mathbf{k}}(\mathbf{r})\Psi^*_{n'\mathbf{k}'}(\mathbf{r}).
\tag{2}
$$

The Fourier transform of the pair density takes the form

$$
\overline{\rho}_{n\mathbf{k},n'\mathbf{k}'}(\mathbf{G}) \equiv \int_{\mathcal{V}} d^3r \left(\rho_{n\mathbf{k},n'\mathbf{k}'}(\mathbf{r})e^{-i(\mathbf{k}-\mathbf{k}')\cdot\mathbf{r}} \right) e^{-i\mathbf{G}\cdot\mathbf{r}}.
\tag{3}
$$

In these expressions, $\mathbf{G}$ denotes a reciprocal lattice vector, $f_{n\mathbf{k}}$ denotes a Brillouin zone weight and occupancy factor, and $\mathcal{V}$ denotes the volume of the unit cell.[12] In addition to evaluating the energy, it is also necessary to evaluate the exchange kernel which takes the form

$$
X_{n\mathbf{k}}(\mathbf{r}) = -\frac{1}{2} \sum_{n'\mathbf{k}'} f_{n'\mathbf{k}'} W_{n\mathbf{k},n'\mathbf{k}'}(\mathbf{r})\Psi_{n'\mathbf{k}'}(\mathbf{r}),
\tag{4}
$$

where the interaction function is defined by

$$
\begin{aligned}
W_{n\mathbf{k},n'\mathbf{k}'}(\mathbf{r}) & \equiv e^2 \int d^3r' \frac{\rho_{n\mathbf{k},n'\mathbf{k}'}(\mathbf{r}')}{|\mathbf{r}-\mathbf{r}'|} \\
& = e^{i(\mathbf{k}-\mathbf{k}')\cdot\mathbf{r}} \sum_{\mathbf{G}} \overline{W}_{n\mathbf{k},n'\mathbf{k}'}(\mathbf{G})e^{i\mathbf{G}\cdot\mathbf{r}}.
\end{aligned}
\tag{5}
$$

The Fourier transform of the interaction kernel given by

$$
\overline{W}_{n\mathbf{k},n'\mathbf{k}'}(\mathbf{G}) = \frac{4\pi e^2}{\mathcal{V}} \frac{\overline{\rho}_{n\mathbf{k},n'\mathbf{k}'}(\mathbf{G})}{|\mathbf{k}-\mathbf{k}'+\mathbf{G}|^2}.
\tag{6}
$$

The numerical challenge of evaluating E_x and $X_{n\mathbf{k}}(\mathbf{r})$ comes in evaluating the singular Brillouin zone integrals in Eqs. (1) and (4) for $|\mathbf{k}-\mathbf{k}'+\mathbf{G}| \to 0$.

II. NUMERICAL TECHNIQUES

A. Singular integration algorithm

A convenient method for numerical evaluation of singular integrals is to introduce an auxiliary function in order to transform the argument of the numerical integral into a non-singular argument. The complete result involves also evaluating the singular integral of the auxiliary function which can be accomplished by using analytic or efficient numerical methods. This idea was first proposed by Gygi and Baldereschi[13] and further developed by Massidda, Posternak, and Baldereschi;[14] several other schemes have appeared in the more recent literature.[3,4,7] Following the work of Duchemin and Gygi[7], Eq. (1) can be evaluated according to

$$
E_x^{\mathrm{D-G}} = -\frac{e^2\pi}{\mathcal{V}} \sum_{n\mathbf{k}} f_{n\mathbf{k}} \left(\mathcal{T}_{n\mathbf{k}}^1 + \mathcal{T}_{n\mathbf{k}}^2 \right),
\tag{7}
$$

where the "principal part"-like discrete summation is defined as

$$
\mathcal{T}_{n\mathbf{k}}^1 \equiv \sum_{n'\mathbf{k}'} f_{n'\mathbf{k}'} \sum_{\mathbf{G}}' \frac{|\overline{\rho}_{n\mathbf{k},n'\mathbf{k}'}(\mathbf{G})|^2 - \delta_{nn'}e^{-\alpha|\mathbf{k}-\mathbf{k}'+\mathbf{G}|^2}}{|\mathbf{k}-\mathbf{k}'+\mathbf{G}|^2}
\tag{8}
$$

and the continuous integral over the auxiliary function is given by

$$
\mathcal{T}_{n\mathbf{k}}^2 \equiv \sum_{n'\mathbf{k}'} f_{n'\mathbf{k}'}\delta_{nn'} \sum_{\mathbf{G}} \frac{e^{-\alpha|\mathbf{k}-\mathbf{k}'+\mathbf{G}|^2}}{|\mathbf{k}-\mathbf{k}'+\mathbf{G}|^2} = \frac{\mathcal{V}}{2\pi\sqrt{\pi\alpha}}.
\tag{9}
$$

The choice of $e^{-\alpha q^2}$ for the auxiliary function is convenient for analytic reasons and it approximates the pair density due to a Bloch band formed from non-overlapping Gaussian orbitals as we will see below.

In order to evaluate the exchange kernel in Eq. (4), we can use a similar approach by evaluating the form

$$
X_{n\mathbf{k}}^{\mathrm{D-G}}(\mathbf{r}) = -\frac{2\pi e^2}{\mathcal{V}} \left(\mathcal{X}_{n\mathbf{k}}^1(\mathbf{r}) + \mathcal{X}_{n\mathbf{k}}^2(\mathbf{r}) \right).
\tag{10}
$$

Here the "principal part"-like discrete summation is performed for the term[15]

$$
\begin{aligned}
\mathcal{X}_{n\mathbf{k}}^1(\mathbf{r}) = & \sum_{n'\mathbf{k}'} f_{n'\mathbf{k}'} \sum_{\mathbf{G}}' \left(\frac{e^{i(\mathbf{k}-\mathbf{k}')\cdot\mathbf{r}}\Psi_{n'\mathbf{k}'}(\mathbf{r})\overline{\rho}_{n\mathbf{k},n'\mathbf{k}'}(\mathbf{G})}{|\mathbf{k}-\mathbf{k}'+\mathbf{G}|^2} \right. \\
& \left. - \delta_{nn'} \frac{\Psi_{n\mathbf{k}}(\mathbf{r})e^{-\alpha|\mathbf{k}-\mathbf{k}'+\mathbf{G}|^2}}{|\mathbf{k}-\mathbf{k}'+\mathbf{G}|^2} \right) e^{i\mathbf{G}\cdot\mathbf{r}}.
\end{aligned}
\tag{11}
$$

The singularity is treated in the term

$$\mathcal{X}_{n\mathbf{k}}^2(\mathbf{r}) = \Psi_{n\mathbf{k}}(\mathbf{r}) \sum_{\mathbf{G}} \overline{\mathcal{G}}_\alpha(\mathbf{G}) e^{i\mathbf{G}\cdot\mathbf{r}}. \tag{12}$$

where the constant function $\overline{\mathcal{G}}_\alpha(\mathbf{G})$ is defined by the Brillouin zone integral

$$\overline{\mathcal{G}}_\alpha(\mathbf{G}) \equiv \sum_{\mathbf{k}'} f_{n\mathbf{k}'} \frac{e^{-\alpha|\mathbf{k}'+\mathbf{G}|^2}}{|\mathbf{k}'+\mathbf{G}|^2}. \tag{13}$$

This function can be evaluated numerically with high accuracy with the help of integration by parts. Specifically, for the case that each band n is doubly occupied, the summation can be expressed as a volume integral over the Brillouin zone $\sum_{\mathbf{k}'} f_{n\mathbf{k}'} \to \frac{2\mathcal{V}}{(2\pi)^3}$ which can be transformed into a smooth volume integral and a non-singular surface integral with the form:

$$\overline{\mathcal{G}}_\alpha(\mathbf{G}) = \frac{2\mathcal{V}}{(2\pi)^3} \left(\int_{\text{BZ (vol)}} d^3k' \, 2\alpha \, e^{-\alpha|\mathbf{k}'+\mathbf{G}|^2} \right.$$
$$\left. + \oint_{\text{BZ (surf)}} d\mathbf{S}_{\mathbf{k}'} \cdot (\mathbf{k}'+\mathbf{G}) \frac{e^{-\alpha|\mathbf{k}'+\mathbf{G}|^2}}{|\mathbf{k}'+\mathbf{G}|^2} \right). \tag{14}$$

This evaluation, while not trivial,[16] is not expected to be the bottleneck of the evaluation of the exchange kernel, particularly since it remains the same throughout the self-consistency iterations of the wavefunctions.

B. Truncated Coulomb kernel algorithm

Spencer and Alavi[4] developed an alternate scheme to evaluate the singularity of the Fock kernel based on adjusting the real-space range of the Coulomb kernel consistent with the $\mathbf{k}$-space integration mesh. In this scheme, the expression for the exchange energy per unit cell takes the form:

$$E_x^{\text{S-A}} = -\frac{e^2\pi}{\mathcal{V}} \sum_{n\mathbf{k}n'\mathbf{k}'} f_{n\mathbf{k}} f_{n'\mathbf{k}'} \sum_{\mathbf{G}} \frac{|\overline{\rho}_{n\mathbf{k},n'\mathbf{k}'}(\mathbf{G})|^2}{|\mathbf{k}-\mathbf{k}'+\mathbf{G}|^2} \tag{15}$$
$$\times (1 - \cos(|\mathbf{k}-\mathbf{k}'+\mathbf{G}|R_c)).$$

Here the cut-off radius R_c is chosen such that $\frac{4\pi}{3}R_c^3 = \mathcal{N}_\mathbf{k}\mathcal{V}$, where $\mathcal{N}_\mathbf{k}$ denotes the number of $\mathbf{k}$-points used in the Brillouin zone integration. The corresponding evaluation of the exchange kernel in this formulation would take the form

$$X_{n\mathbf{k}}^{\text{S-A}}(\mathbf{r}) = -\frac{1}{2} \sum_{n'\mathbf{k}'} f_{n'\mathbf{k}'} W_{n\mathbf{k},n'\mathbf{k}'}^{\text{S-A}}(\mathbf{r}) \Psi_{n'\mathbf{k}'}(\mathbf{r}), \tag{16}$$

where

$$W_{n\mathbf{k},n'\mathbf{k}'}^{\text{S-A}}(\mathbf{r}) \equiv e^{i(\mathbf{k}-\mathbf{k}')\cdot\mathbf{r}}$$
$$\times \sum_{\mathbf{G}} \overline{W}_{n\mathbf{k},n'\mathbf{k}'}(\mathbf{G})\left[1 - \cos(|\mathbf{k}-\mathbf{k}'+\mathbf{G}|R_c)\right]e^{i\mathbf{G}\cdot\mathbf{r}}. \tag{17}$$

III. NUMERICAL EXAMPLE

By analyzing these algorithms for a simple analytic model, we can assess some of the properties of the algorithms in detail. This, together with tests on "real" materials that have appeared in the literature,[2–5,7–9] will help refine the computational approaches.

A. Simple analytic model

We imagine a system with a single site per unit cell and with a single band, filled with one electron of each spin, and described by localized spherically symmetric Gaussian orbital of the form

$$\phi_n(r) \equiv \frac{1}{(\pi a^2)^{3/4}} \, e^{-\frac{1}{2}(r/a)^2}. \tag{18}$$

Here a denotes a length parameter which we will assume is substantially smaller than any of the lattice constants of the crystal. A Bloch-wave of wavevector $\mathbf{k}$ can be constructed from linear combinations of the localized orbital:

$$\Psi_{n\mathbf{k}}(\mathbf{r}) = \sum_\mathbf{T} e^{i\mathbf{k}\cdot\mathbf{T}} \phi_n(|\mathbf{r}-\mathbf{T}|), \tag{19}$$

where $\mathbf{T}$ denotes a lattice translation. For this model, assuming that the orbitals are non-overlapping, the pair density function is given by in real space by

$$\rho_{n\mathbf{k},n\mathbf{k}'}(\mathbf{r}) \approx \sum_\mathbf{T} e^{i(\mathbf{k}-\mathbf{k}')\cdot\mathbf{T}} |\phi_n(|\mathbf{r}-\mathbf{T}|)|^2. \tag{20}$$

The Fourier transform of the pair density is given by

$$\overline{\rho}_{n\mathbf{k},n\mathbf{k}'}(\mathbf{G}) \approx e^{-|\mathbf{k}-\mathbf{k}'+\mathbf{G}|^2 a^2/4}. \tag{21}$$

For this model, the exchange energy per unit cell has the analytic result

$$E_x = -\frac{e^2}{a}\sqrt{\frac{2}{\pi}}, \tag{22}$$

and the exchange kernel can be expressed in terms of error functions:

$$X_{n\mathbf{k}}(\mathbf{r}) = -e^2 \sum_\mathbf{T} e^{i\mathbf{k}\cdot\mathbf{T}} \phi_n(|\mathbf{r}-\mathbf{T}|) \frac{\text{erf}(\frac{|\mathbf{r}-\mathbf{T}|}{a})}{|\mathbf{r}-\mathbf{T}|}. \tag{23}$$

From this very simple analytic model, we are now in a position to evaluate the numerical properties of several evaluation algorithms discussed in the literature.

B. Numerical results for the model system

In order to perform the numerical study, we chose $a = 1$ bohr and constructed simple cubic lattices with cube lengths $L = 8$ bohr to ensure that the overlap error is no more than
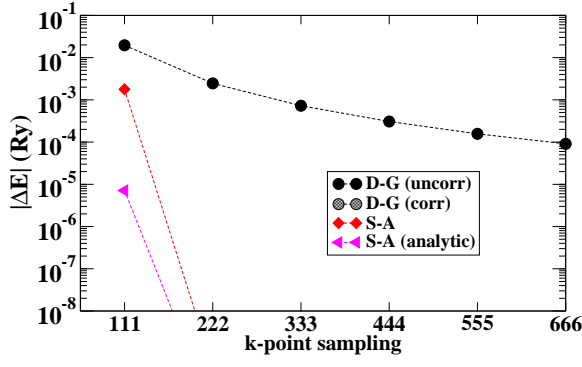
FIG. 1. (Color online.) Magnitude of the exchange energy differences relative to exact result (22), calculated using the Duchemin-Gygi ("D-G") and Spencer-Alavi ("S-A") schemes. The horizontal axis represents the $\mathbf{k}$-point sampling in terms of the partitioning numbers $N_1 N_2 N_3$. Note that results for the "D-G (corr)" scheme do not show up on the plot.

10^{-7}. The Brillouin zone was sampled by partitioning the primitive reciprocal cell into N_1, N_2, and N_3 segments, with $\mathcal{N}_{\mathbf{k}} \equiv N_1 N_2 N_3$, so that the weight factors take the values $f_{n\mathbf{k}} = \frac{2}{\mathcal{N}_{\mathbf{k}}}$. The sampling $\mathbf{k}$-points are chosen to have the values

$$\mathbf{k}_i = f_1^i \mathbf{G}_1 + f_2^i \mathbf{G}_2 + f_3^i \mathbf{G}_3, \qquad (24)$$

where $\mathbf{G}_1, \mathbf{G}_2, \mathbf{G}_3$ denote the primitive reciprocal lattice vectors and the the fractional components are given by

$$f_1^i = -\frac{1}{2} + \frac{x_i - \frac{1}{2}}{N_1} \quad \text{where} \quad 1 \leq x_i \leq N_1. \qquad (25)$$

Figure 1 illustrates the errors in the exchange energy E_x for the various algorithms. Results for the Duchemin-Gygi method do depend on the choice of α, but for $\alpha \neq a^2/2$, the trends are very similar; $\alpha = 0.1$ bohr^2 is used here. The label D-G (uncorr) refers to the auxiliary function method described in Sec. II A where the singular point is omitted from the sum. These results converge relatively slowly with $\mathbf{k}$-point sampling, and can be shown to be dominated "curvature" error $\propto \frac{\alpha - a^2/2}{\mathcal{N}_{\mathbf{k}}}$. In order to improve this convergence, Duchemin and Gygi[7] suggested a better treatment of the integrand of Eq. (8) in the neighborhood of the singularity, which for the model system evaluates to

$$\lim_{|\mathbf{k}-\mathbf{k}'+\mathbf{G}|\to 0} \left[\frac{|\bar{\rho}_{n\mathbf{k},n'\mathbf{k}'}(\mathbf{G})|^2 - \delta_{nn'}\mathrm{e}^{-\alpha|\mathbf{k}-\mathbf{k}'+\mathbf{G}|^2}}{|\mathbf{k}-\mathbf{k}'+\mathbf{G}|^2} \right] = \alpha - \frac{a^2}{2}, \qquad (26)$$

which is labeled D-G (corr) in Fig. 1, but is in fact too close to the exact result to show up on the plot.

The numerical results of Fig. 1 show that the Spencer-Alavi scheme (Sec. II B) converges faster than the uncorrected Duchemin-Gygi method. Because we have an analytic form for the pair density function, we can evaluate the integral (15) without considering the sampling error of the numerical integration.

$$E_x^{\mathrm{S-A}} = -\frac{e^2}{a}\sqrt{\frac{2}{\pi}}\left(1 - \mathrm{e}^{-R_c^2/(2a^2)}\right). \qquad (27)$$
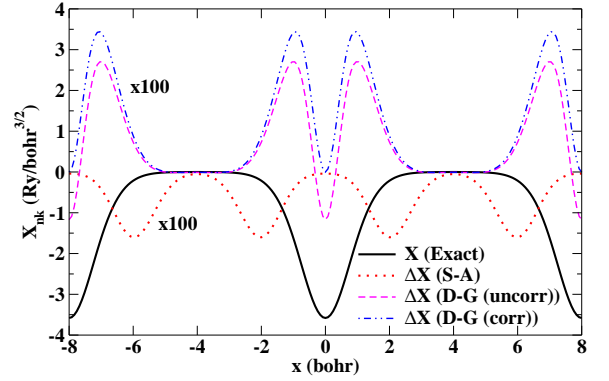

FIG. 2. (Color online.) Plot of the exact exchange kernel function $X_{n\mathbf{k}}(\mathbf{r})$ for $\mathbf{k} = 0$ plotted along a cube edge, compared with the numerical differences obtained using single $\mathbf{k}$-point sampling with the approximations of Spencer and Alavi ($\Delta X \equiv X_{n\mathbf{k}}^{\mathrm{S-A}} - X_{n\mathbf{k}}$) and Duchemin and Gygi ($\Delta X \equiv X_{n\mathbf{k}}^{\mathrm{D-G}} - X_{n\mathbf{k}}$). To help the visualization, the exchange kernel differences ("ΔX") have been multiplied by 100.

This shows that for any choice of $\mathcal{N}_{\mathbf{k}}$ for the $\mathbf{k}$-point integration mesh and its corresponding cut-off radius R_c, there is an error factor of $\mathrm{e}^{-R_c^2/(2a^2)}$. Fortunately, this term is typically very small and decreases further with increasing $\mathcal{N}_{\mathbf{k}}$, as illustrated in Fig. 1 with the label "S-A (analytic)".

We have also investigated the calculation of the exchange kernel function $X_{n\mathbf{k}}(\mathbf{r})$ as shown in Fig. (2) using the various algorithms and the case of a single $\mathbf{k}$-point sampling. Here we see that the errors of all of the methods are in the 1% range. The spatial distribution of the errors is different for Duchemin-Gygi and Spencer-Alavi algorithms. For the Duchemin-Gygi case, the curvature correction to the integrand (10) in the limit $|\mathbf{k} - \mathbf{k}' + \mathbf{G}| \to 0$ changes the shape of the error, but does not drastically reduce its magnitude as it did for the calculation of the energy. We have checked the algorithm for larger $\mathbf{k}$-point samplings and find the results to converge to the exact $X_{n\mathbf{k}}(\mathbf{r})$ at a rate similar to that of the convergence of E_x in the uncorrected Duchemin-Gygi method. For the Spencer-Alavi method, the single $\mathbf{k}$-point sampling gives a small oscillatory error. For the simple model, the Spencer-Alavi modified exchange kernel (16) can be evaluated analytically apart from the $\mathbf{k}$-point sampling error with the result

$$X_{n\mathbf{k}}^{\mathrm{S-A}}(\mathbf{r}) = -e^2 \sum_{\mathbf{T}} \mathrm{e}^{i\mathbf{k}\cdot\mathbf{T}} \phi_n(|\mathbf{r}-\mathbf{T}|)$$

$$\times \left[\frac{\mathrm{erf}(\frac{|\mathbf{r}-\mathbf{T}|}{a})}{|\mathbf{r}-\mathbf{T}|} - \frac{\mathrm{erf}(\frac{R_c+|\mathbf{r}-\mathbf{T}|}{a}) - \mathrm{erf}(\frac{R_c-|\mathbf{r}-\mathbf{T}|}{a})}{2|\mathbf{r}-\mathbf{T}|} \right]. \qquad (28)$$

The difference of this result from the exact kernel (23) for the case illustrated in Fig. (2) is essentially zero for all arguments on the scale of the plot.

C. Gamma point approximations

In modeling systems with large supercells or modeling molecules or clusters using periodic boundary conditions, it is convenient to limit the Brillouin zone sampling to a single $\mathbf{k}$-point, typically the Γ point.[5,9] The present model falls into the same category as these systems, since we have assumed non-overlapping orbitals. Even for our case where the overlap is less than 10^{-7}, we see that Γ-point sampling can introduce an error due to unphysical interactions between unit cells. To analyze the origin of the unphysical interaction, we can write the exchange energy (1) in terms of sums of real-space integrals

$$E_x = -e^2 \sum_{\mathbf{k}\mathbf{k}'} \sum_{\mathbf{T}} e^{i(\mathbf{k}-\mathbf{k}')\cdot\mathbf{T}} \mathcal{T}_{\mathbf{T}}, \tag{29}$$

where, for the Gaussian model, the interaction term is

$$\mathcal{T}_{\mathbf{T}} \equiv \int d^3r \, \frac{\mathrm{erf}(r/a)}{r} e^{-|\mathbf{r}-\mathbf{T}|^2/a^2}. \tag{30}$$

Comparing this expression with the analytic results given in Eq. (22), it is apparent that only the on-site term $\mathcal{T}_{\mathbf{T}=0}$ contributes to the physical result. However, using the Γ point sampling to approximate the Brillouin zone sampling over $\mathbf{k}$ and $\mathbf{k}'$, the exchange energy expression becomes

$$E_x^{\Gamma} = -e^2 \sum_{\mathbf{T}} \mathcal{T}_{\mathbf{T}}, \tag{31}$$

showing that the unphysical interaction terms contribute to the numerical result. This analysis is consistent with the larger errors for the "111" $\mathbf{k}$-point sampling results shown in Fig. 1 and, by extension, for the 1% errors shown in Fig. 2. For-tunately, the unphysical $\mathcal{T}_{\mathbf{T}\neq0}$ contributions decrease with increasing simulation cell size. In the exact expression, the Brillouin zone integration provides suppression of contributions from different cells due the interference integral:

$$\sum_{\mathbf{k}} e^{i\mathbf{k}\cdot\mathbf{T}} = \delta_{\mathbf{T}0}. \tag{32}$$

While Γ-point sampling contributes no interference, finite Brillouin zone sampling contributes some interference effects and thus improves the numerical result. An attractive alternative method of avoiding unphysical exchange interactions between localized states might be to use a Wannier function representation as has been suggested by Wu, Selloni, and Car.[6]

IV. SUMMARY AND CONCLUSIONS

The simple model presented in this work exercises some of the challenges of evaluating Fock exchange and provides an interesting test system which has helped us evaluate algorithms and implementations. In particular, we have been able to show that in the plane-wave basis, $\mathbf{k}$-point sampling can be important even for systems with large unit cells. Both the Duchemin-Gygi[7] and Spencer-Alavi[4] algorithms are shown to work well for the test system.

ACKNOWLEDGMENTS

* natalie@wfu.edu; http://www.wfu.edu/~natalie

[1] S. Sharma, J. K. Dewhurst, and C. Ambrosch-Draxl, Phys. Rev. Lett. **95**, 136402 (2005).

[2] A. Sorouri, W. M. C. Foulkes, and N. D. M. Hine, J. Chem. Phys. **124**, 064105 (7pp) (2006).

[3] P. Carrier, S. Rohra, and A. Görling, Phys. Rev. B **75**, 205126 (10pp) (2007).

[4] J. Spencer and A. Alavi, Phys. Rev. B **77**, 193110 (4pp) (2008).

[5] P. Broqvist, A. Alkauskas, and A. Pasquarello, Phys. Rev. B **80**, 085114 (13pp) (2009).

[6] X. Wu, A. Selloni, and R. Car, Phys. Rev. B **79**, 085102 (5pp) (2009).

[7] I. Duchemin and F. Gygi, Computer Physics Communications **181**, 855 (2010).

[8] J. Harl, L. Schimka, and G. Kresse, Phys. Rev. B **81**, 115126 (18pp) (2010).

[9] E. J. Bylaska, K. Tsemekhman, S. B. Baden, J. H. Weare, and H. Jonsson, Journal of Computational Chemistry **32**, 54 (2011).

[10] M. Betzinger, C. Friedrich, S. Blügel, and A. Görling, Phys. Rev. B **83**, 045105 (11pp) (2011).

[11] In order for the planewave expansions to converge, a pseudopotential or augmented plane wave formulation must generally be used.

[12] The expression assumes (for simplicity) a spin unpolarized system.

[13] F. Gygi and A. Baldereschi, Phys. Rev. B **34**, 4405 (1986).

[14] S. Massidda, M. Posternak, and A. Baldereschi, Phys. Rev. B **48**, 5058 (1993).

[15] Previous formulations of the exchange kernel (such as in Ref. 2 and 3), are expressed in terms of double reciprocal lattice summations. In the current formulation, the evaluation of Eq. (10) can be accomplished by carrying out non-singular summations over $\mathbf{G}$ using Fast Fourier Transforms and accumulating the results in $\mathbf{r}$ space.

[16] Both the volume and surface integrals can be evaluated numerically by using fractional coordinates in the reciprocal lattice basis and Gaussian quadrature.